

# Modeling the Unconventional Superconducting Properties of Expanded $A_3C_{60}$ Fullerides

Massimo Capone,<sup>1,2</sup> Michele Fabrizio,<sup>3,4</sup> Claudio Castellani,<sup>1</sup> and Erio Tosatti<sup>3,4</sup>

<sup>1</sup>*SMC, CNR-INFM and Dipartimento di Fisica, Università "La Sapienza", P.le Aldo Moro 2, I-00185, Roma, Italy*

<sup>2</sup>*ISC-CNR, Via dei Taurini 19, I-00185 Roma, Italy*

<sup>3</sup>*International School for Advanced Studies (SISSA), and CNR/INFM DEMOCRITOS National Simulation Center, Via Beirut 2-4, I-34014 Trieste, Italy*

<sup>4</sup>*The Abdus Salam International Center for Theoretical Physics (ICTP), P.O.Box 586, I-34014 Trieste, Italy*

(Dated: November 2, 2018)

The trivalent alkali fullerides solids of generic composition  $A_3C_{60}$ , where  $C_{60}$  is the fullerene molecule and  $A = K, Rb, \text{ and } Cs$ , are a well established family of molecular superconductors. The superconductive electron pairing is of regular  $s$ -wave symmetry and is accounted for by conventional coupling of electrons to phonons, in particular by well understood Jahn Teller intramolecular  $C_{60}$  vibrations. A source of renewed interest in these systems are alarming indications of strong electron-electron repulsion phenomena, which emerged especially in compounds where the  $C_{60}$ - $C_{60}$  distance is expanded, by either a large cation size or by other chemical or physical means. Several examples are now known where this kind of expansion, while leading to a high superconducting temperature at first, gradually or suddenly causes a decline of superconductivity and its eventual disappearance in favor of a Mott insulating state. This kind of insulating state is the hallmark of strong electron correlations in cuprate and organic superconductors, and its appearance suggests that fullerides might also be members at large of that family.

Our approach to the fullerides is theoretical, and based on the solution of a Hubbard type model, where electrons hop between molecular sites. We take advantage of the fact that, unlike models for the strongly correlated cuprates, still under debate, in a Hubbard model of fullerides all the important electron correlations occur within the molecular site, efficiently soluble in the Dynamical Mean Field Theory (DMFT) approximation. DMFT solutions confirm that superconductivity in this model fulleride, although of  $s$ -wave symmetry rather than  $d$ -wave, shares many of the properties that are characteristic of high  $T_c$  cuprates. The calculations are heavy; and while our working model is several years old, the new results we present in this Colloquium pertain to the most interesting case of three electrons per  $C_{60}$  molecule, appropriate to  $A_3C_{60}$ , and have only been possible recently thanks to a stronger computational effort.

We have calculated the zero temperature phase diagram as a function of the ratio of intra-molecular repulsion parameter  $U$  over the electron bandwidth  $W$ , the increase of  $U/W$  representing the main effect of lattice expansion. The phase diagram is close to that of actual materials, with a dome shaped superconducting order parameter region preceding the Mott transition for increasing cell volume. Unconventional properties of expanded fulleride superconductors predicted by this model include: (i) an energy pseudogap in the normal phase; (ii) a gain of electron kinetic energy and of conducting Drude weight at the onset of superconductivity, as in high  $T_c$  cuprates; (iii) a spin susceptibility and a specific heat behavior that is not drastically different from a regular phonon superconductor, despite strong correlations; (iv) the emergence of more than one energy scale governing the renormalized single particle dispersion, electronic entropy and the specific heat jump. These predictions, which if confirmed should establish fullerides, especially the expanded ones, as members of the wider family of strongly correlated superconductors, are discussed in the light of existing and foreseeable experiments.

PACS numbers: 71.30+h, 71.10.Pm, 71.10.Fd

<b>Contents</b>		<b>Superconductivity from DMFT and the Impurity Model</b>	9
<b>I. introduction</b>	2	A. Anderson Impurity With a Rigid Bath	11
<b>II. Electron Interactions in Fullerides</b>	3	B. Anderson Impurity with a Self-Consistent Bath in DMFT	12
<b>III. Model and Interactions</b>	5	<b>V. Discussion of Experimental Probes</b>	13
A. Dynamical Mean-Field Theory	5	<b>VI. Conclusions</b>	15
B. $T = 0$ Phase Diagram	7	<b>Acknowledgments</b>	16
<b>IV. Understanding Strongly Correlated</b>			

## I. INTRODUCTION

Discovered by Kamerlingh Onnes nearly a century ago (Onnes, 1911), and first explained microscopically back in 1957 in terms of electron pairing by Bardeen, Cooper and Schrieffer (BCS) (Bardeen *et al.*, 1957a,b), superconductivity is still surprisingly *a' la page*. On one hand, superconductivity is being constantly discovered in an ever increasing variety of solid state compounds. On the other hand, it appears more and more difficult to use basically the same standard theory, essentially BCS and its extensions (e.g. Parks, 1969, chapters 10 and 11) to account for all of them. In this standard, conventional theory, superconductivity arises from the condensation of electron pairs, the two electrons usually bound in a pair state of *s*-wave symmetry and held together by exchange of lattice phonons. The Coulomb repulsion between the two electrons opposes pair formation, but it does not suppress superconductivity because screening makes it weak enough.

The surprisingly favorable effect of repulsive electron correlations on superconductivity found in some systems, particularly in high- $T_c$  superconducting cuprates, where electron-electron repulsion is dominant, remains a standing puzzle. An immense amount of experimental and theoretical work has accumulated over the last two decades in the attempt to understand these phenomena, see e.g. the review by Bennemann and Ketterson (2008). Actually, cuprates are but the most spectacular members of a wider class of strongly correlated superconductors including heavy fermion and organic molecular compounds (Bennemann and Ketterson, 2008), systems for which there is no really comprehensive theory either. Among other factors, theoretical efforts have been hampered by the general *inter-site* nature of electron interactions and correlations in many of these systems, a fact that poses large technical difficulties. In this light, identifying a superconductor family where correlations are at the same time strong, simple, and *on-site* is welcome.

A more crucial element is one of perspective. It has been a widespread prejudice to distinguish between superconductors where (as in BCS theory) pairing of electrons takes place in the *s*-wave channel and is mediated by phonons, from those where the mechanism may be electronic and not phononic, and where pairing instead takes place in the *d*-wave channel. Whereas it is widely held that strong repulsive correlations are essential to superconductivity in the latter (Anderson, 1987), they are not considered crucial in the former. The conventional BCS scenario and its extensions, namely the Migdal-Eliashberg theory (Eliashberg, 1960; Migdal, 1958; Parks, 1969) – a controlled approximation valid when the typical phonon frequency is much smaller than the Fermi energy – are more or less automatically accepted, and used to account for the superconducting properties. In

this theory, electron-electron repulsion merely renormalizes the electron-phonon parameters, lowering the critical temperature  $T_c$  rather than enhancing it.

The trivalent alkali fullerides superconductors, excellently reviewed, e.g., by Gunnarsson (1997, 2004) and Ramirez (1994), are among the systems where this conventional logic seemingly applies. Fullerides are solid state compounds of generic composition  $A_3C_{60}$ , where  $C_{60}$  is the fullerene molecule (Gunnarsson, 2004) and  $A = K, Rb,$  and  $Cs$  are alkali cations. The three alkalis donate a total of  $n=3$  electrons to each fullerene, half filling its threefold degenerate  $t_{1u}$  molecular level. Electron hopping between first neighboring fullerenes gives rise to a metal, where conduction is restricted to the three narrow  $t_{1u}$ -derived bands, with a total energy bandwidth of no more than 0.6 eV (Erwin, 1993; Satpathy *et al.*, 1992). Metallic fullerides are generally superconducting, with critical temperatures  $T_c$  reaching  $\sim 40$  K, depending on various factors. An empirically important factor appears to be the cell volume. When the fulleride lattice is chemically expanded, by either increasing cation size or by insertion of neutral molecules, or else physically expanded by removing pressure,  $T_c$  undergoes a definite and systematic change. It rises initially with a good correlation with the  $C_{60}$ - $C_{60}$  distance (Gunnarsson, 1997; Yildirim *et al.*, 1995). Further expansion however causes  $T_c$  to drop, ending eventually, through a first order transition, in an insulating state, as we shall discuss later.

A wealth of evidence indicates that superconducting pairing in fullerides is phononic and that the relevant phonons are the stiff intra-molecular  $H_g$  vibrations of the  $C_{60}$  molecule, Jahn-Teller coupled to the  $t_{1u}$  conduction electrons (Gunnarsson, 1997). Further support to the apparent BCS nature of superconductivity in fullerides comes from specific-heat jumps that scale linearly with  $T_c$  in agreement with BCS theory (Burkhart and Meingast, 1996; Kortan *et al.*, 1992; Ramirez, 1994), as well as a regular (i.e., not exceedingly high) normal phase magnetic susceptibility. (Kortan *et al.*, 1992; Robert *et al.*, 1998) Superconducting energy gaps are less clearly defined, (Gunnarsson, 1997) the gap ratio  $2\Delta/T_c \simeq 3.4 - 4.2$  in  $K_3C_{60}$  and  $Rb_3C_{60}$  (Gunnarsson, 1997; Ramirez, 1994), but not far from the BCS value of 3.53. These elements suggest viewing the  $A_3C_{60}$  compounds as weakly correlated Fermi-liquid conductors (Ramirez, 1994), though with unusually narrow electron bands, with a large effective mass roughly three free electron masses (Robert *et al.*, 1998). Even the observed decrease of  $T_c$  under applied pressure in  $K_3C_{60}$  and  $Rb_3C_{60}$  is in qualitative agreement with an increasing bandwidth and decreasing density of states at the Fermi level, which further supports a standard BCS picture.

These reassuring, conventional looking facts are however contrasted by a number of conflicting elements that are strong enough to cast serious doubts on the general applicability of the BCS scenario to superconductors in this family. These elements are especially apparent in the more expanded ful-

lerides including  $(\text{NH}_3)_x\text{NaK}_2\text{C}_{60}$  (Riccó *et al.*, 2003) and  $\text{Li}_3\text{C}_{60}$  (Durand *et al.*, 2003), and in the alloys  $\text{Cs}_{3-x}\text{K}_x\text{C}_{60}$  and  $\text{Cs}_{3-x}\text{Rb}_x\text{C}_{60}$  (Dahlke *et al.*, 2000). For these expanded compounds  $T_c$  decreases upon expansion, contrary to BCS theory. The electron density of states extracted by NMR Knight shift is at the same time an increasing function of lattice parameter, smoothly connecting with that of the unalloyed compounds under pressure (Dahlke *et al.*, 2000). Within BCS theory, that increase should lead to a rise of  $T_c$  and not to a drop as observed. The same unconventional behavior is observed in  $\text{Cs}_3\text{C}_{60}$ , the fulleride compound with the highest  $T_c \sim 40$  K attained under pressure (Palstra *et al.*, 1995). A novel A15 superconducting phase of  $\text{Cs}_3\text{C}_{60}$  with expanded structure has very recently been synthesized (Ganin *et al.*, 2008) corresponding to a body-centered cubic arrangement of fullerenes. Superconductivity emerges under pressure through a first order non-structural transition at 4 Kbar. The critical temperature  $T_c$  first increases with pressure, reaching a dome-shaped maximum of 38 K around 7 Kbar, above which  $T_c$  drops. Since no structural changes are observed under pressure, the appearance of superconductivity as well as the dome-shaped  $T_c$  vs. pressure behavior must be ascribed solely to the volume contraction (Ganin *et al.*, 2008). This non-monotonic behavior of  $T_c$  with pressure finds no apparent explanation within the conventional theory.

The basic and striking anomaly of expanded fullerides occurs in the compounds with the largest inter-molecule distances. In these materials a relatively modest additional lattice expansion (and minor change of symmetry due to intercalated ammonia) is enough to dramatically turn them from metallic and superconducting to antiferromagnetic and insulating (Durand *et al.*, 2003; Iwasa and Takenobu, 2003).<sup>1</sup> With temperature, antiferromagnetic order in the ammoniated compound  $\text{NH}_3\text{K}_3\text{C}_{60}$  changes to paramagnetic disorder at a Néel temperature slightly above  $\sim 40$  K (Prassides *et al.*, 1999). Even above the Néel temperature, the microwave conductivity in  $\text{NH}_3\text{K}_3\text{C}_{60}$  remains several orders of magnitude below that of  $\text{K}_3\text{C}_{60}$  (Kitano *et al.*, 2002), testifying the Mott insulator (correlation driven) nature of the insulating phase. Electrons in a lattice give rise to a Mott insulating state when electron-electron repulsion stops their free propagation and the lattice appears as a collection of molecular ions. Correlations lead to an energy gap in their spectrum, even if their number density per cell is odd, instead of even as in regular band insulators (Mott, 1990). Proximity of a Mott insulator phase in fullerides had long been advocated in different contexts (Baskaran and Tosatti, 1991; Chakravarty *et al.*, 1991; Chakravarty and Kivelson, 1991; Lof *et al.*, 1992)

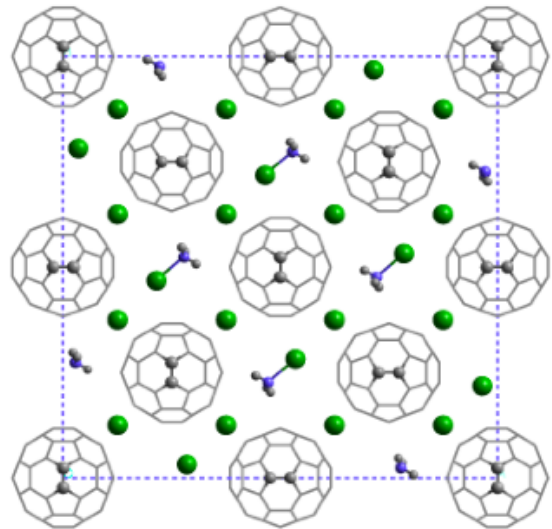


FIG. 1 Schematic representation of a planar projection of the crystal structure of  $\text{NH}_3\text{K}_3\text{C}_{60}$ . Green dots are potassium atoms, blue dots surrounded by three grey dots are  $\text{NH}_3$  molecules, and  $\text{C}_{60}$  molecules are shown according to their actual spatial orientation. (Courtesy of Kosmas Prassides).

but was not taken seriously by the community prior to this data. Superconductivity next to a Mott insulating phase as a function of doping or volume change is the hallmark of strong correlations in high temperature superconducting cuprates and organics. One is thus naturally led to inquire whether superconductivity in expanded fullerides might, despite the obvious differences, and despite the phononic mechanism, be somehow related to strong correlations. Our contention is that it is indeed closely related, as outlined in the following.

## II. ELECTRON INTERACTIONS IN FULLERIDES

The electrons donated by the alkalis to the  $\text{C}_{60}$  molecule enter the threefold degenerate  $t_{1u}$  former lowest unoccupied molecular orbital (LUMO). In a degenerate molecular orbital, electrons interact through a variety of mechanisms. The first is overall Coulomb repulsion, which we will associate later below with the Hubbard parameter  $U$ . The second is Coulomb exchange energy, minimized when the molecular state has the highest total spin, and the highest total orbital angular momentum compatible with it (Hund's rules) (Landau and Lifshitz, 1958). The third is the Jahn-Teller (JT) interaction, caused by coupling of the electron levels to symmetry lowering molecular distortions (Landau and Lifshitz, 1958, chap. 13). Contrary to Hund's rules, in a JT distorted molecule the ground state maximizes double occupancy of levels, thus favoring low total spin instead of high spin in the isolated

<sup>1</sup> We expect that below the superconducting pressure of 4 kbar, the new compound A15  $\text{Cs}_3\text{C}_{60}$  (Ganin *et al.*, 2008), yet to be characterized in this respect, should also be an insulating antiferromagnet.

molecular ion. In molecular  $C_{60}^{3-}$ , the strength of these interactions has been evaluated in the past, and the JT strength has been estimated to prevail narrowly over Hund's rule exchange (Lüders *et al.*, 2002). This narrow balance favors a low-spin ground state, with a relatively small "spin gap" – the energy between the low spin ground state and the lowest high-spin excited state, expected to be of the order of 0.1 eV (Capone *et al.*, 2001; Lüders *et al.*, 2002). In agreement with this expectation, local moments indicate that in antiferromagnetic Mott insulating  $NH_3K_3C_{60}$  the  $C_{60}(3-)$  sites are in a *low-spin* state,  $S = 1/2$  (Prassides *et al.*, 1999), their high spin state  $S = 3/2$  lying about 100 meV higher in energy. A low-spin qualifies the overexpanded fullerenes as "Mott-Jahn-Teller" insulators – that is, Mott insulators whose sites are in a JT stabilized low-spin state (as opposed to a Hund's rule stabilized high-spin state) (Fabrizio and Tosatti, 1997). Under hydrostatic pressure,  $NH_3K_3C_{60}$  undergoes a transition to a metallic state where superconductivity re-emerges with a rather large  $T_c$  (Prassides *et al.*, 1999). It is important to note that this superconducting phase still belongs to the "expanded" family, as signaled by the fact the  $T_c$  here *increases* further with increasing pressure (reaching 28 K at 14.8 kbar (Zhou *et al.*, 1995)) at variance with non-expanded fullerenes, where  $T_c$  drops under pressure.

A lateral, but relevant additional element comes from *tetravalent* compounds  $A_4C_{60}$ , which are insulators or near insulators. By comparison with the trivalent fullerenes, the slight reduction of band-energy gain per particle caused by adding one more electron per molecule and by slightly changing the crystal structure is sufficient to turn the trivalent metals into tetravalent insulators even in non-expanded materials. Careful density-functional electronic structure calculations indicated that it is not possible to describe the tetravalent compounds such as  $K_4C_{60}$  as statically distorted Jahn-Teller band insulators (Capone *et al.*, 2000). A static JT distortion and the associated orthorhombic state is actually present only in  $Cs_4C_{60}$  (Dahlke and Rosseinsky, 2002), and in  $Rb_4C_{60}$  above a critical pressure (Huq and Stephens, 2006), while it never shows up in  $K_4C_{60}$  (Huq and Stephens, 2006) (with the exception of monolayers, see Wachowiak *et al.* (2005)). The persistence of insulating or near insulating behavior and the recovery of molecular symmetry observed in the high temperature phase of tetravalent fullerenes suggests that these compounds too are Mott-Jahn-Teller insulators (Capone *et al.*, 2000; Klupp *et al.*, 2006; Knupfer and Fink, 1997), like the overexpanded trivalent materials. The dynamic JT effect in each  $C_{60}^{4-}$  ion associated with Mott localization of carriers is crucial in explaining the low spin ground state and the spin gap of  $A_4C_{60}$ , exactly as for the expanded trivalent compounds.

From the above discussion one might be tempted to conclude that strong correlations play a role only in tetravalent and expanded trivalent compounds, while face-centered cubic (f.c.c.)  $K_3C_{60}$  and  $Rb_3C_{60}$ , where su-

perconductivity was originally discovered, could still be viewed as weakly correlated systems, and as BCS type superconductors. We do not believe in this conclusion. A final, independent and strongly unconventional signal is provided by NMR. In fact, NMR data show direct evidence of a spin gap of order 0.1 eV, appearing as an anomalous activated increase of inverse relaxation time. Most likely this gap between a low spin ground state and a high spin excited state reflects the multiplet behavior of the localized  $C_{60}^{n-}$  molecular ion. It shows up ubiquitously in all alkali doped fullerenes, including superconducting f.c.c. compounds (Brouet *et al.*, 2002a,b; Thier *et al.*, 1995). The existence of the spin gap signifies that the magnetic response of fullerenes is very far from Fermi-liquid behavior, which has no such feature. Magnetically, the fullerenes behave as if localized molecular multiplet excitations coexisted with delocalized propagating quasiparticles. As discussed, the recovery of molecular physics is characteristic of Mott insulators, suggesting that the fingerprint of Mott physics is strongly present already in the non-expanded superconducting f.c.c. compounds. This suggests that the f.c.c. compounds are somehow the analog of the overdoped cuprates, whereas the expanded trivalent materials are analogous to the underdoped cuprates. The conclusion is that both are crucially, even if differently, influenced by electron correlations.

We believe that the above elements are strong enough to call for a new physical picture for the whole family of  $A_3C_{60}$  superconductors. Proximity of the Mott insulator strongly suggests that the anomalies of expanded fullerene superconductors most likely originate from strong repulsive electron correlation in the narrow  $t_{1u}$  bands. The prevalence in the Mott localized state of molecular physics, with its orbital degeneracy, JT effect and intra-molecular exchange must be taken into account along with itinerant electron band physics. Upon expanding the cell volume, the intermolecular hopping of electron weakens, whereas all the on-site correlation terms – Coulomb and exchange electron-electron interactions as well as molecular JT effect – are likely to become increasingly relevant. We are led to a picture where the Mott insulator physics of weakly coupled molecular ions progressively prevails over band physics for increasing lattice expansion. In particular, superconductors that operate in this regime are bound to deviate from the standard Migdal-Eliashberg scenario, the more so as the lattice spacing increases. To investigate that regime, we need to start with a broader theoretical scheme for trivalent fullerenes, capable of describing their behavior under lattice expansion and near the Mott transition. While that has been the scope of our work for several years, previous work was for practical technical reasons limited to tetravalent systems (Capone *et al.*, 2002, 2000, 2001). The study of  $A_3C_{60}$  systems, computationally much heavier due to the simultaneous relevance of magnetic and orbital ordering, has only now been completed, and we offer here an outline of the main results.

### III. MODEL AND INTERACTIONS

Our theoretical model of trivalent fullerides assumes a lattice of molecular sites, each representing a  $C_{60}$  molecule. The  $C_{60}$   $t_{1u}$  threefold degenerate LUMO can for all purposes be treated as an atomic  $p$  level. An average of three electrons per molecule are donated by alkali atoms and partially fill these orbitals, which can host up to six electrons. The electrons hop from site to site giving rise to half-filled bands of width  $W \sim 0.6\text{eV}$ . On each site the electrons experience a Hubbard repulsion  $U \sim 1\text{eV}$  (corresponding to the Slater integral  $F_0 \propto U$ ),

$$\mathcal{H}_U = \frac{U}{2} (n - 3)^2, \quad (1)$$

together with a weaker, yet crucial, inter-orbital Hund's rule exchange coupling term  $J_H$  proportional to the Slater integral  $F_2$ . Under the sole assumption of full rotational orbital symmetry, this exchange term takes the form (Capone *et al.*, 2002, 2001)

$$\mathcal{H}_J = J \left( 2\mathbf{S} \cdot \mathbf{S} + \frac{1}{2}\mathbf{L} \cdot \mathbf{L} \right) + \frac{5}{6} J (n - 3)^2, \quad (2)$$

where  $J = -J_H < 0$ , while  $n$ ,  $\mathbf{S}$  and  $\mathbf{L}$  are the density, spin and orbital angular momentum operators, defined as for  $p$ -orbitals, on the given site. This exchange term favors high  $\mathbf{S}$  and  $\mathbf{L}$  molecular multiplets, and has been overlooked or neglected in most treatments so far. The next interaction is the JT intra-molecular coupling of electrons in the  $t_{1u}$  orbital to  $H_g$  intra-molecular vibrations. This interaction has on the contrary been very widely discussed (see e.g. Auerbach *et al.* (1994); Gunnarsson *et al.* (1995); Lannoo *et al.* (1991); Varma *et al.* (1991) and references therein), and we will not dwell too much on its details here. It acts to split the  $t_{1u}$  orbital degeneracy and thus favors low spin states, effectively playing the opposite role to intra-molecular exchange. A proper treatment of the JT coupling involves the dynamics of carbon nuclei in  $C_{60}^{n-}$  ions, including retardation, and has been developed by Gunnarsson *et al.* (1995) However for expanded fullerides close enough to the Mott transition, retardation is not essential and can be omitted. In fact, in this regime the inter-site motion of quasiparticles is severely slowed down (Georges *et al.*, 1996) and the coherent bandwidth will eventually drop from  $W$  to  $ZW$  ( $Z \ll 1$ ). When  $ZW$  falls enough to approach the relatively high  $H_g$  vibration frequencies of fullerene  $\hbar\omega \sim 90\text{meV}$  (Capone *et al.*, 2002, 2000, 2001), quasiparticles begin to move on a comparable time scale with the vibrating carbon atoms, and non-adiabatic effects become important (Cappelluti *et al.*, 2000). Even closer to the Mott transition, the phonon dynamics becomes eventually *faster* than inter-molecular quasiparticle hopping. In this anti-adiabatic limit, molecular vibrations can be integrated away, and the resulting unretarded effective JT interaction recovers identically the same form as Hund's rule exchange (2) except for the sign

of  $J$ , namely  $J_{JT} > 0$  (Capone *et al.*, 2001). In this limit the Hund and JT intra-molecular inter-orbital interaction terms can be directly combined in the form (2) with  $J = -J_H + J_{JT}$ . In  $C_{60}$ ,  $J_H \simeq 0.03 - 0.1\text{eV}$  (Lüders *et al.*, 2002; Martin and Ritchie, 1993), whereas  $J_{JT} \simeq 0.06 - 0.12\text{eV}$  (Auerbach *et al.*, 1994; Gunnarsson *et al.*, 1995; Lannoo *et al.*, 1991; Lüders *et al.*, 2002; Varma *et al.*, 1991). The total result – and the only one compatible with s-wave superconductivity, with a spin 1/2 Mott insulator, and with a moderate spin gap near 0.1 eV – is a relatively weak unretarded attraction which has the form of an *inverted* Hund's rule coupling (Capone *et al.*, 2002; Granath and Östlund, 2003). This is the approximation we shall adopt, keeping in mind that it is strictly valid only when  $ZW < \hbar\omega$ , that is, close enough to the Mott transition.

The lattice expansion characterizing the expanded fullerides is believed to have little effect on either  $J_H$  or  $J_{JT}$ . On the other hand, expansion will surely decrease  $W$  and increase  $U$ , so it can be modeled as a gradual increase of  $U/W$ , reflecting both the band narrowing due to smaller overlap between molecular wave functions, and a decreased screening strength. As discussed above, this Hamiltonian model, even if not really simple, has many body interactions that are strictly on site, an ideal situation for Dynamical Mean-Field Theory (DMFT) (Georges *et al.*, 1996), one of the most popular and powerful tools in the field of strongly correlated electron systems that we briefly describe in the next subsection.

#### A. Dynamical Mean-Field Theory

DMFT is a quantum version of classical mean-field theory, which provides an exact description of the local dynamics, at the price of freezing away all spatial fluctuations. The mean-field scheme is formulated by a mapping of the lattice model onto an Anderson impurity model (AIM) embedded in a free-electron Fermi “bath” subject to a self-consistency condition (Georges *et al.*, 1996). In our model, the effective AIM is three-fold orbitally degenerate, with p-like levels representing the  $t_{1u}$  orbitals, each hybridized with a bath. The Hamiltonian is

$$\mathcal{H} = \mathcal{H}_U + \mathcal{H}_J + \sum_{ka\sigma} \varepsilon_{ka} c_{ka\sigma}^\dagger c_{ka\sigma} + \sum_{ka\sigma} V_{ka} (c_{ka\sigma}^\dagger p_{a\sigma} + H.c.), \quad (3)$$

where  $\mathcal{H}_U$  and  $\mathcal{H}_J$  are (1) and (2) for fermions on the impurity orbitals,  $\varepsilon_{ka}$  are the bath energy levels labeled by the index  $k$  and by an orbital index  $a = x, y, z$ ,  $V_{ka}$  are the hybridization parameters between the bath fermions, created by  $c_{ka\sigma}^\dagger$ , and the impurity fermions, created by  $p_{a\sigma}^\dagger$ . The mean-field scheme implies a self-consistency condition that depends on the impurity Green's function and on the bare density of states of the original lattice. Throughout our calculations, we use an infinite-coordination Bethe lattice, whose density of states is

semicircular. This is a reasonable description of a realistic three-dimensional density of states devoid of accidental features such as van-Hove singularities. It is moreover particularly convenient since it leads to a very simple and transparent form of the self-consistency condition. The Bethe lattice is the  $z \rightarrow \infty$  limit of a Cayley tree of coordination  $z$ , scaling the nearest-neighbor hopping in each one of the  $z$  directions as  $t/\sqrt{z}$ . The resulting semicircular density of states has bandwidth  $= 4t$ .

The self-consistency condition requires the so-called Weiss field (i.e., the non-interacting Green's function of the AIM)

$$\mathcal{G}_0^{-1}(i\omega_n)_a = (i\omega_n + \mu) - \sum_k \frac{V_{ka}^2}{i\omega_n - \varepsilon_{ka}}, \quad (4)$$

to be related to the local interacting Green's function,  $G_a(i\omega_n)$ , not only through the Dyson equation for the AIM

$$\mathcal{G}_0^{-1}(i\omega_n)_a = G_a^{-1}(i\omega_n) + \Sigma_a(i\omega_n),$$

which requires the full solution of the impurity model, but also by the additional selfconsistency equation

$$\mathcal{G}_{0a}^{-1}(i\omega_n) = (i\omega_n + \mu) - t^2 G(i\omega_n)_a. \quad (5)$$

DMFT for a given model thus amounts to solve iteratively the AIM until the impurity Green's function satisfies Eq. (5). In this work, we solved the threefold degenerate AIM by exact diagonalization. That requires truncating the sum over  $k$  in Eqs. (3) and (5) to a finite and relatively small number of baths  $N_b$ , so that the Hamiltonian can be diagonalized in the finite resulting Hilbert space. We generally used  $N_b = 4$  for each orbital. Most of the results we shall present are at zero temperature, where we can use the Lanczos algorithm to calculate the Green's function without fully diagonalizing the Hamiltonian. The finite temperature results for the specific heat and its jump at  $T_c$  reported in Sec. V are the exception. They are obtained by means of the finite-temperature extension of Lanczos (Capone *et al.*, 2007), where the thermal Green's function is expressed as a sum over the low-lying eigenvectors  $|n\rangle$  and eigenvalues  $E_n$  of the impurity model

$$G_{a\sigma}(i\omega_n) = \frac{1}{Z} \sum_m e^{-\beta E_m} G_{a\sigma}^{(m)}(i\omega_n) \quad (6)$$

with

$$G_{a\sigma}^{(m)}(i\omega_n) \equiv \sum_n \frac{|\langle n|p_{a\sigma}|m\rangle|^2}{E_m - E_n - i\omega_n} + \sum_n \frac{|\langle n|p_{a\sigma}^\dagger|m\rangle|^2}{E_n - E_m - i\omega_n}. \quad (7)$$

The Boltzmann factor in Eq. (6) guarantees that the lower the temperature, the smaller the number of excited states that actually contribute to the Green's function. Therefore, for sufficiently low temperature, we can

still use the Lanczos algorithm to find the lowest energy eigenstates. In practice, only a limited number of states,  $20 \div 25$ , can be calculated in a reasonable time. Unfortunately, this number is insufficient to make the truncation error in Eq. (6) negligible for the present model in the relevant correlated regime. We estimate the systematic error on the Green's function to be of order of a few per cent, a level of accuracy that does not allow to fully determine thermodynamic properties such as the critical temperature. Luckily though, this error affects much more the absolute specific heat value than its relative changes, including the superconducting jump in units of  $T_c$  which we shall discuss further below (see Sec. V). We underline that this limitation does not affect by any means the  $T = 0$  calculations.

The above DMFT equations refer to a paramagnetic phase where no symmetry breaking occurs. However, in this work we shall be crucially interested in  $s$ -wave superconducting and in antiferromagnetic solutions, where symmetry is broken. Superconductivity is conveniently studied in the Nambu-Gor'kov representation by introducing spinors

$$\psi_{\mathbf{k}a} = \begin{pmatrix} p_{\mathbf{k}a\uparrow} \\ p_{-\mathbf{k}a\downarrow}^\dagger \end{pmatrix},$$

and defining accordingly the Green's function  $G_{\mathbf{k}a}(\tau) = -\langle T_\tau (\psi_{\mathbf{k}a}(\tau) \psi_{\mathbf{k}a}^\dagger(0)) \rangle$  in imaginary time as a  $2 \times 2$  matrix that satisfies the Dyson equation in Matsubara frequencies

$$G_{\mathbf{k}a}(i\omega) = G_{\mathbf{k}a}^0(i\omega) + G_{\mathbf{k}a}^0(i\omega) \Sigma(i\omega) G_{\mathbf{k}a}(i\omega), \quad (8)$$

with  $G_{\mathbf{k}a}^0(i\omega)$  the non-interacting value. The single-particle self-energy  $\Sigma(i\omega)$  is also a  $2 \times 2$  matrix whose off-diagonal element  $\Delta(i\omega)$ , when finite, signals a superconducting phase. The DMFT self-consistency can be written now as

$$\mathcal{G}_0^{-1}(i\omega_n) = i\omega_n \tau_0 + \mu \tau_3 - t^2 \tau_3 G(i\omega_n) \tau_3, \quad (9)$$

where  $\tau_0$  and  $\tau_3$  are Pauli matrices.

Analogously, antiferromagnetism in a bipartite lattice is conveniently described using the spinor

$$\psi_{\mathbf{k}a\sigma} = \begin{pmatrix} p_{\mathbf{k}a\sigma} \\ p_{\mathbf{k}+\mathbf{Q}a\sigma} \end{pmatrix},$$

with  $\mathbf{k}$  in the magnetic Brillouin zone and  $\mathbf{Q}$  the modulation vector. This leads once more to a  $2 \times 2$  Green's function and self-energy matrices related by the Dyson equation (8). Here too, a finite off-diagonal element signals an antiferromagnetically ordered phase. The self-consistency equation for antiferromagnetism exploits the bipartite property of the lattice. Indicating one sublattice with A and the other with B, the general self-

consistency condition is

$$\mathcal{G}_0^{-1}(i\omega_n)_{\sigma A} = (i\omega_n + \mu) - t^2 G(i\omega_n)_{\sigma B}, \quad (10)$$

which becomes Eq. (5) if  $G_{\sigma A} \equiv G_{\sigma B}$ , i.e. if the system is nonmagnetic. When the system is antiferromagnetic, then  $G_{\sigma A} \equiv G_{-\sigma B}$ . Thus we can eliminate the sublattice B from Eq. (10), and obtain the following result for the self-consistency equation:

$$\mathcal{G}_0^{-1}(i\omega_n)_{\sigma A} = (i\omega_n + \mu) - t^2 G(i\omega_n)_{-\sigma A}. \quad (11)$$

This equation is valid for a Bethe lattice with nearest neighbor hopping, a case with perfect nesting that is rather exceptional in realistic antiferromagnets. A way to simulate imperfect nesting typical of more realistic situations, while still taking advantage of the Bethe-lattice simplifications, is to add a next-nearest-neighbor hopping  $t'/z$  in the Cayley tree (merely a device to eliminate nesting, not meant to suggest next nearest neighbor hopping, small in fullerenes). In the limit  $z \rightarrow \infty$  of the Bethe lattice, the self-consistency equation becomes

$$\begin{aligned} \mathcal{G}_0^{-1}(i\omega_n)_{\sigma A} &= (i\omega_n + \mu) - t^2 G(i\omega_n)_{\sigma B} - t'^2 G(i\omega_n)_{\sigma A} \\ &= (i\omega_n + \mu) - t^2 G(i\omega_n)_{-\sigma A} - t'^2 G(i\omega_n)_{\sigma A} \end{aligned}$$

For both broken-symmetry phases, if the diagonal elements of the self-energy matrix at low Matsubara frequencies follow the conventional Fermi-liquid behavior – which we always find to be the case,

$$\Sigma_{diagonal}(i\omega_n) \simeq \left(1 - \frac{1}{Z}\right) i\omega_n, \quad (13)$$

the actual value of the spectral gap in the single particle spectrum is given by  $Z \Delta(0)$ , the zero frequency anomalous (superconducting or antiferromagnetic) self-energy multiplied by the so-called quasiparticle weight  $Z$ .

We end by noting that, within DMFT, one can search for solutions with different symmetries by simply allowing/preventing symmetry breaking order parameters, even in regions where the chosen phase is not the most stable. When two or more solutions coexist, the stable one is determined by an explicit energy calculation. As we shall discuss, for a wide range of  $U/W$  values we do find coexisting superconducting and antiferromagnetic solutions, the former prevailing at smaller  $U$ , the latter at larger  $U$ . The physical phase diagram thus exhibits a first-order transition between these two symmetry broken phases – a nonmagnetic  $s$ -wave superconductor, and an insulating spin 1/2 antiferromagnet – taking place when the respective energy curves intersect.

## B. $T = 0$ Phase Diagram

Modeling lattice expansion of fullerenes as a gradual increase of  $U/W$ , we can proceed to analyze the theoretical zero temperature “phase diagram” of our model obtained

by DMFT as a function of  $U/W$ . Starting with the uncorrelated system with  $U = 0$  the model initially exhibits straight BCS superconductivity driven by JT phonons (i.e., the attractive  $J$  we introduced above) with an  $s$ -wave ( $S = L = 0$ ) order parameter<sup>2</sup>

$$P_{SC} = \frac{1}{N} \sum_i \sum_{a=x,y,z} \langle p_{i a \uparrow}^\dagger p_{i a \downarrow}^\dagger \rangle, \quad (14)$$

where  $N$  is the number of molecules and  $p_{i a \sigma}^\dagger$  creates an electron on molecule  $i$ , with spin  $\sigma$  and in orbital  $a = x, y, z$ . The Fermi-liquid scattering amplitude in the Cooper channel, measuring the strength of the effective attraction, is  $A = -10J/3$ . We note that owing to fairly strong JT interactions (Auerbach *et al.*, 1994; Gunnarsson *et al.*, 1995), if Hund’s exchange  $J_H$  were neglected, the dimensionless JT coupling constant of fullerene controlling superconductivity would be numerically very large,  $\lambda = \rho_0 |A| \simeq 0.6 - 1.0$ , where  $\rho_0$  ( $\simeq 2.4 \text{ eV}^{-1}$ ) is the bare density of states per spin and orbital. Turning on a weak Coulomb repulsion  $U$  on top of that will reduce the pairing attraction in this regime. Perturbatively one obtains for small  $U$  that  $A = -10J/3 + U$ . Since  $J$  is insensitive to expansion while  $U/W$  increases, this implies that in this picture, where Hund’s rule exchange is neglected,  $T_c$  should always *decrease* upon expansion, a prediction which is at odds with experiments.

In fact, as anticipated, Hund’s rule exchange is not negligible, and its effect is to introduce a substantial cancellation in  $J$  leading to a largely reduced effective coupling  $\lambda_{eff} \simeq \frac{10}{3} (J_{JT} - J_H) \rho_0$ . Should we interpret the ubiquitous spin gap of 0.1 eV (Brouet *et al.*, 2002a,b; Thier *et al.*, 1995) as the  $C_{60}^{n-}$  molecular excitation energy between its low spin ground state with  $S = 1/2$  and  $S = 0$  for  $n = 3$  and  $n = 4$ , respectively, and its high spin excited state, with  $S = 3/2$  and  $S = 1$  for  $n = 3$  and  $n = 4$ , respectively, we would conclude that, to be consistent with our model where both gaps are equal to  $5J$  (Capone *et al.*, 2004), the total effective inverted exchange  $J$ , comprehensive of both JT and Hund’s rule exchange, should be approximately  $J = 0.02 \text{ eV}$ . In reality, the qualitative scenario we will describe is relatively independent of the precise value of  $J$  provided it is inverted, i.e., negative and small.

Once exchange is included, the resulting  $\lambda_{eff} \simeq 0.16$  is now much smaller – in fact way too small to explain within conventional BCS or Migdal-Eliashberg theory any of the observed values of  $T_c$  in fullerenes (let alone the non-monotonic behavior of  $T_c$  versus the density of states for expanded fullerenes (Dahlke *et al.*, 2000; Ganin *et al.*, 2008)). Things get worse when we increase the on-site Coulomb repulsion  $U$  closer to realistic values,  $U \sim W$

<sup>2</sup> Since gauge symmetry is broken, we are allowed to assume  $P_{SC}$  real

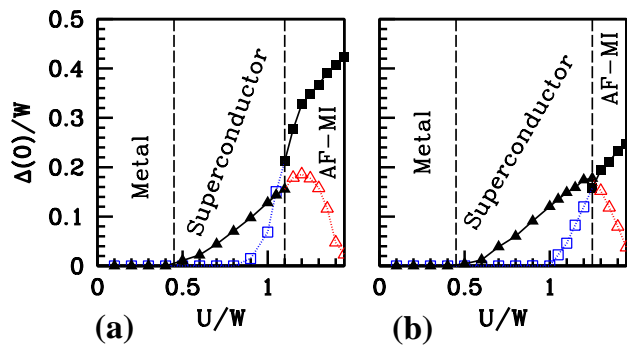


FIG. 2 Superconducting solution (triangles) and antiferromagnetic solution (squares) zero-frequency anomalous self-energies  $\Delta(0)$  as function of  $U/W$ . Solid symbols are used when the corresponding symmetry broken phase is stable, while open symbols when it is metastable, i.e. has lower energy than the other phase. The first-order transition between the two phases is indicated by a vertical line separating the superconductor from the antiferromagnetic Mott insulator. Panel (b) corresponds to the case in the presence of a frustrating next-nearest neighbor hopping  $t' = 0.3t$ , absent in (a).

and beyond. In the conventional weakly correlated picture  $U$  would provide in the electron pairing problem a repulsive “Coulomb pseudopotential” whose bare value is  $\mu_* = U \rho_0 \simeq 3$  (Parks, 1969). Simply comparing these bare values of  $\lambda$  and  $\mu_*$  we should conclude that  $s$ -wave BCS superconductivity in fullerenes is simply impossible (with the obvious proviso that for small  $U$  an unretarded treatment of JT phonon interactions is not really justified).

The full DMFT solution of the model for  $J = 0.05 W$  and increasing  $U/W$  yields the phase diagram in Fig. 2. While confirming the above expectations for moderate  $U$ , it has a surprise in reserve at larger  $U$  values, where the Mott transition is approached.

Fig. 3 shows the zero frequency anomalous single-particle self-energies calculated within DMFT for the superconducting and for the antiferromagnetic solution. At  $U = 0$ , the model is an  $s$ -wave BCS superconductor, with an exponentially small superconducting  $\Delta(0)$ . It is too small to be visible in the figure, since the effective exchange-reduced  $\lambda \sim 0.2$  is as was said very weak. Beginning from zero, the increase of  $U$  first rapidly destroys the weak BCS superconductivity. The superconducting  $\Delta(0)$  vanishes at roughly the mean-field value  $U = 10/3J$ , and above this value of  $U$  the ground state becomes a normal metal as expected. Upon further increasing  $U/W$  the model remains a normal metal – no superconductivity, no antiferromagnetism. However, the importance of electron correlations increases with  $U$ , as signaled for example in the DMFT spectral function (not shown) by the gradual formation of incoherent Hubbard bands on both sides of the Fermi level. The metallic character persists until a hypothetically continuous Mott

transition eventually reached near  $U/W \sim 1.5$ , where  $Z = 0$  and the metallic character is extinguished.

Before this happens however,  $s$ -wave superconductivity re-enters from the normal metal state. The anomalous self energy  $\Delta(0)$ , proportional to the superconducting order parameter has, as a function of  $U$ , a bell-shaped behavior – a “superconducting dome” as it is called in cuprates – hitting a large maximum before dropping again. The re-entrant superconductive behavior is a clear realization of phonon-induced strongly correlated superconductivity (SCS) (Capone *et al.*, 2002). The sharply rising order parameter edge with increasing  $U/W$  can in our view explain the strong rise of  $T_c$  upon lattice expansion in non-expanded compounds, previously (and we believe incorrectly) attributed to a BCS-like increase of density of states upon band narrowing. Past the dome maximum, and upon increasing expansion, the SCS superconducting order parameter declines, and would eventually drop to zero at the continuous metal insulator transition near  $U/W \sim 1.5$ . This continuous decline of superconductivity is preempted by a first order transition to a lower energy antiferromagnetic Mott insulating phase, with order parameter

$$P_{AFM} = \frac{1}{N} \sum_i (-1)^i (n_{i\uparrow} - n_{i\downarrow}), \quad (15)$$

where  $n_{i\sigma} = \sum_{a=x,y,z} p_{i a \sigma}^\dagger p_{i a \sigma}$  is the full occupation number with spin  $\sigma$  at molecule  $i$ . The exact location of the superconductor-insulator transition depends on details. For strong nesting ( $t'=0$ ) it takes place even before the superconducting dome maximum. In Fig. 3 we show  $\Delta(0)$  of Fig. 2 in comparison with the spectral gaps  $Z\Delta(0)$ , as well as the order parameters  $P_{SC}$  and  $P_{AFM}$ . Notice that  $Z$  for the superconductor is smaller and vanishes at the continuous metal insulator transition, while  $Z$  for the antiferromagnet is of order 1. In both cases the dimensionless order parameter essentially follows the behavior of the spectral gap.

When we add a next-nearest neighbor hopping  $t'$  to mimic imperfect nesting (as we expect to find generically for realistic band structures, in particular in the face-centered cubic  $A_3C_{60}$  materials), we find that the superconducting phase is only weakly affected but antiferromagnetism is strongly frustrated. As a result the superconducting region expands at expense of the magnetic insulator, and the superconducting dome may emerge in full [panel (b) of Fig. 2]. We propose that the gradual drop of superconducting order parameter past the dome maximum now naturally explains the decline of  $T_c$  of expanded fullerenes (Dahlke and Rosseinsky, 2002; Durand *et al.*, 2003; Ganin *et al.*, 2008).

Finally, past the first-order Mott transition, we find that the antiferromagnetic insulator is formed mainly by spin-1/2 local configurations, which is in agreement with experiments in  $NH_3K_3C_{60}$  (Iwasa and Takenobu, 2003). We also predict that ambient pressure  $A_{15}Cs_3C_{60}$ , yet to be characterized, should similarly be a

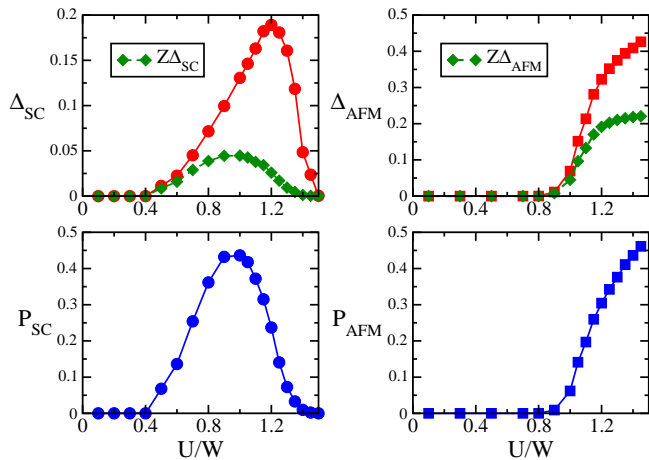


FIG. 3 Superconducting solution (SC, left) and antiferromagnetic solution (AFM, right) anomalous self-energies (top) and order parameters (bottom) as a function of  $U/W$ . The top panels also show (green diamonds) the spectral gaps obtained multiplying  $\Delta$  by the quasiparticle weight  $Z$  of each solution. The gaps are in units of the bandwidth  $W$  (the order parameters are by definition dimensionless). Dashed vertical lines mark the first-order phase transition between the two solutions.

spin-1/2 antiferromagnetic insulator. Besides spin rotational symmetry, this kind of state also breaks orbital rotational symmetry, signaling that spin ordering must be generally accompanied by orbital ordering. In ammoniated fullerenes that again is consistent with experiment (Iwasa and Takenobu, 2003). We conclude that, in spite of strong simplifying assumptions, our model seems able to reproduce very important features of the phase diagram of expanded fullerenes. In the following we shall discuss in more detail the strongly correlated superconducting phase near the Mott transition, and also propose experiments that might distinguish it from a standard BCS state.

#### IV. UNDERSTANDING STRONGLY CORRELATED SUPERCONDUCTIVITY FROM DMFT AND THE IMPURITY MODEL

The re-emergence of phonon-driven superconductivity close to the Mott transition – Strongly Correlated Superconductivity (SCS) – was discussed in Capone *et al.* (2002) in terms of Fermi-liquid theory. A key point of that phenomenon is the renormalization of the effective bandwidth and thus of the effective mass, both controlled (in a Bethe lattice) by the quasiparticle weight  $Z$ , Eq. (13).  $Z(U)$  decreases as a function of  $U/W$  and vanishes at the continuous metal insulator transition point  $U = U_c$ , where the effective mass  $m^*/m = 1/Z(U)$  diverges, and the effective quasiparticle bandwidth  $W_* = ZW$  vanishes. An estimate of the interaction between charged quasiparticles requires the evolution of fluctuations that take place in charge space. Because charge

fluctuations are gradually frozen away near the Mott transition, the effective repulsion between quasiparticles is also renormalized down to some smaller value  $U_* < U$ . In particular, the Fermi-liquid description provided, e.g., by the Gutzwiller variational approach (Gutzwiller, 1963) and supported by the DMFT behavior of the average charge fluctuations  $\langle(n-3)^2\rangle$ , suggests that  $U_* \simeq U \Gamma_U Z(U)^2 \sim U Z(U)$ , where  $\Gamma_U$  includes all the so-called vertex corrections (Abrikosov *et al.*, 1965). This implies that the vertex function  $\Gamma_U$  diverges close to the Mott transition, but does not compensate the vanishing of  $Z$  (Capone *et al.*, 2002). The pairwise Jahn-Teller and exchange based attraction  $J$  between quasiparticles, even if small, here is restricted to spin and orbital space, and has nothing to do with charge fluctuations. In other words, Hund’s rule exchange and the JT coupling only influence the internal splitting of each molecular multiplet without affecting its center of gravity. As a result, this attraction should remain unrenormalized  $J_* = J \Gamma_J Z(U)^2 \sim J$  close to the metal insulator transition, thus implying a strongly divergent vertex correction  $\Gamma_J$  that cancel the vanishing  $Z$ . Therefore the electron pair scattering amplitude  $A_*$  in the Cooper channel should renormalize as  $A = U - \frac{10}{3}J \rightarrow A_* = Z(U)U - \frac{10}{3}J$ . When  $U/W$  is small,  $Z \lesssim 1$ , the main effect of  $U$  is to suppress superconductivity, as was noted earlier. However, if  $U$  is close to the critical metal-insulator value  $U_c$ , then  $Z \sim (U_c - U)/U_c \ll 1$  and the scattering amplitude turns negative in spite of a large  $U$ . This is qualitatively the reason for the SCS re-entrance of superconductivity (though in this region of course the actual pair scattering amplitude might deviate from this simple formula (Capone *et al.*, 2002)).

In addition, the Fermi-liquid argument suggests an explanation for the large value of superconducting order parameter, implying a large  $T_c$ , in the SCS regime, see Fig. 2, compared to the  $U = 0$  BCS values. In fact, when  $A_* \simeq ZW$ , and  $Z$  is dropping sharply, the quasiparticle attraction  $A_*$  will at some point  $U = U_*$  equal the coherent quasiparticle bandwidth  $ZW$ . That very uncommon situation, of metallic quasiparticles with an pair attraction equal to their energy bandwidth, is known to yield maximum superconductivity for a given attraction. As shown by studies of purely attractive models (Micnas *et al.*, 1990), the maximum superconducting temperature  $k_B T_c$  attainable in that case is about 7% of the pair attraction energy itself. In our model of trivalent fullerenes, this estimate yields  $k_B T_c \sim 0.07 A_* \sim 0.2 |J|$ , which has the correct magnitude of roughly 40 K for  $J \sim 20$  meV – a value in turn fully consistent with the observed spin gap  $0.1$  eV  $\sim 5J$ . While this coincidence of numbers is probably fortuitous, it does indicate that orders of magnitude implied by our model with realistic parameters are quite consistent with experimental facts. At face value, it also suggests that  $0.07 |J| = 0.07 (J_{JT} - J_H)$  could be the maximum attainable  $k_B T_c$  in fullerenes. We conclude that strong correlations play a crucial role in bringing the superconducting gap magnitude to the right

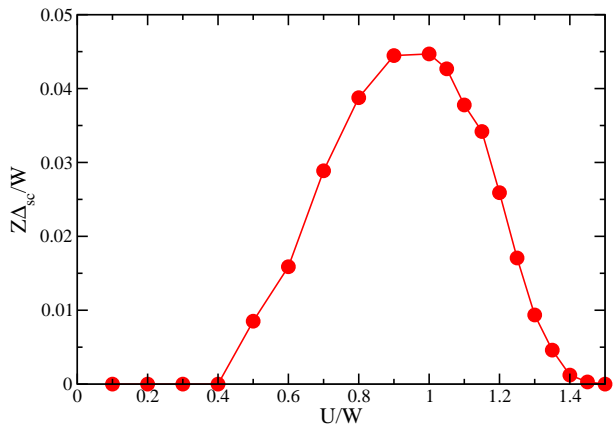


FIG. 4 Quasiparticle superconducting energy gap in units of the bandwidth  $W \simeq 0.6$  eV and on a larger scale than Fig. 3, computed through the anomalous self-energy, panel (a) in Fig. 2, multiplied by the quasiparticle residue  $Z(U)$ . Notice that, above  $U/W \simeq 1.1$ , the superconducting solution is metastable since the antiferromagnetic one has lower energy, see Fig. 2. We note that the maximum gap  $Z\Delta_c \simeq 0.045 W \simeq 27$  meV.

range of values as compared with the experimental ones, see Fig. 4. Such values and large critical temperatures would never be attained within conventional BCS theory using a value of  $\lambda \simeq 0.16 - 0.2$ , including as it should the large cancellation of JT by exchange. They could in point of fact be attained if the cancellation due to exchange were (incorrectly) neglected; but then a lattice expansion should always lead to a decrease of  $T_c$ , contrary to experiment.

To appreciate further the effect of exchange-JT cancellation, it is instructive to consider, as was done for a simplified model by Capone *et al.* (2004), the behavior with  $U/W$  of the superconducting self-energy  $\Delta(0)$  (proportional to the  $T = 0$  gap, and roughly speaking to  $T_c$ ) starting with pure JT and without exchange, and then proceeding to turn on exchange and gradual cancellation, see Fig. 5. For the bare JT,  $\lambda \simeq 1$  (a strong coupling value) the superconducting self-energy decreases monotonically with increasing  $U$ , in agreement with the Migdal-Eliashberg prediction of an increasing Coulomb pseudo-potential. Above a critical value, the system turns directly, via a second-order or weakly first-order phase transition, to a Mott insulating phase. This result is fully consistent with previous calculations by Han *et al.* (Han *et al.*, 2003), where the same type of Hubbard model was studied within DMFT at finite temperature. Treating explicitly the electron-phonon coupling (including the full phonon dynamics) with  $\lambda = 0.6$  and neglecting exchange they obtained a superconductor with monotonically decreasing gap.

Through a progressive reduction of  $\lambda$  (mimicking JT cancellation by exchange) we find that a non-monotonic superconducting behavior makes its appearance as a function of  $U$ . Initially there is still a single superconducting phase for all  $U/W$  values; but two differ-

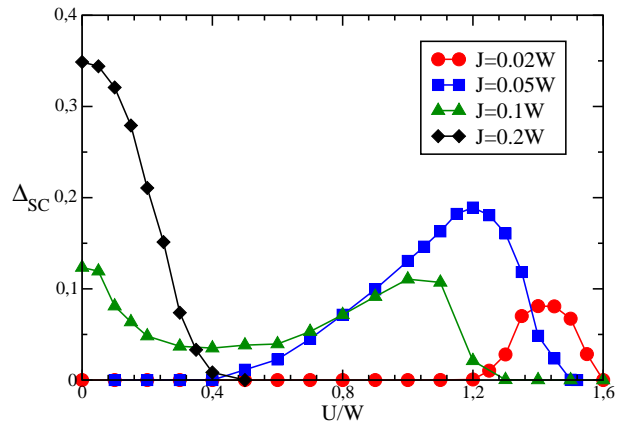


FIG. 5 Anomalous self-energy  $\Delta(0)$  (related to the superconducting gap by a factor  $Z^{-1}$ ) for the superconducting solution and different values of the coupling parameter  $J = 0.02, 0.05, 0.1$  and  $0.2$ , which correspond to  $\lambda = 0.09, 0.21, 0.42, 0.85$ , respectively. Note that for large  $J$ , corresponding to a case where the Jahn Teller coupling is not canceled by Hund's rule exchange, superconductivity is strongest at  $U = 0$ . For increasing cancellation (decreasing  $J$ ), two separate superconducting pockets emerge, a BCS pocket near  $U = 0$ , and a SCS pocket near the Mott insulator. When the cancellation is nearly complete, SCS is many orders of magnitudes stronger than BCS. This is the situation we propose in our model of fullerenes. Similar physics was described for a simpler model in Capone *et al.* (2004).

ent regions near zero and near  $U_c$  begin to materialize. (Note that  $U_c$  simultaneously shifts to higher  $U$  as  $\lambda$  decreases). When the cancellation is so strong that  $\lambda$  is still positive but small, the two superconducting regions break apart to form two separate pockets, leaving a normal metal phase in between. In the leftmost pocket near  $U/W = 0$  the anomalous self-energy has a BCS-like exponential dependence on  $\lambda$  and indeed superconductivity in this corner is BCS. Superconductivity in the rightmost pocket near the metal insulator transition behaves quite differently. Here the  $\lambda$  dependence of superconductivity is much weaker, and the superconductive gap much stronger, than in the BCS pocket. Superconductivity in this pocket can in fact be characterized as SCS (Capone *et al.*, 2002), due to narrow quasiparticle pairing as described above. A similar behavior to Fig. 5, with two separate BCS and SCS regimes emerging from a single initial one when the effective pairing attraction is progressively weakened by exchange, was derived and illustrated in a simpler twofold degenerate model in Capone *et al.* (2004).

The SCS superconducting pocket near the Mott transition is expected to differ from the BCS pocket even in its normal state properties. The normal state underlying a BCS superconductor is Fermi-liquid-like. On the other hand, previous analysis suggest that the Fermi-liquid picture is likely to break down in our model when the Mott transition is approached. The key reason for the breakdown of the Fermi-liquid is precisely that, when

$Z \rightarrow 0$ , the attraction between quasiparticles must eventually reach and exceed in magnitude the quasiparticle bandwidth  $ZW$ , a situation difficult to sustain.<sup>3</sup> Possible deviations from the Fermi-liquid paradigm were in fact overlooked in Ref. (Capone *et al.*, 2002) as they are related to the very-low energy behavior of the normal phase close to the Mott transition, not explored in that work. Later, the non-Fermi-liquid behavior was discovered in the two-orbital model where the physics is very similar (Capone *et al.*, 2004).

### A. Anderson Impurity With a Rigid Bath

The DMFT calculations described above involved two steps, one solving the Anderson impurity model (AIM), the other making that selfconsistent with the bath. Following a reasoning proposed by Fabrizio *et al.* (2003), one may start off with the first step alone, namely analyzing the bare AIM without imposing any self-consistency constraint. The conduction bath can be assumed to have a flat density of states, and the bath-impurity hybridization to be structureless, a situation which avoids numerical uncertainties and yields accurate low-energy properties. This kind of analysis applied to the AIM (3) shows (De Leo and Fabrizio, 2005) that two different impurity phases are stabilized according to the ratio between the attraction  $J$ , and the Kondo temperature  $T_K$  (Hewson, 1997). Below this temperature and when  $J = 0$ , the spin of an impurity coupled to a Fermi sea is screened out and absorbed in the conduction sea (Hewson, 1997). In the lattice context within DMFT, the Kondo scale measures metallic coherence and corresponds to the renormalized quasiparticle bandwidth  $ZW$ . For finite  $J \neq 0$  but smaller than  $T_K$ , Kondo screening remains, thus still implying a Fermi-liquid behavior in DMFT. In fullerenes, the impurity represents the  $C_{60}^{3-}$  ion, carrying three orbitals and three spins. In the Kondo phase each of the three spins is separately screened by the bath and thus incorporated in the Fermi sea. Conversely, when  $J > T_K$  the Kondo screening is lost, and that was shown to imply a non Fermi-liquid phase characterized by a pseudogap in the single-particle spectrum and by several other singular properties (De Leo and Fabrizio, 2005). A very qualitative description of this phase is that, unlike the Kondo phase, two spins out of three pair off antiferromagnetically at any given time, leaving out a single spin 1/2 available for Kondo screening. However, since orbital degeneracy is unbroken, this residual

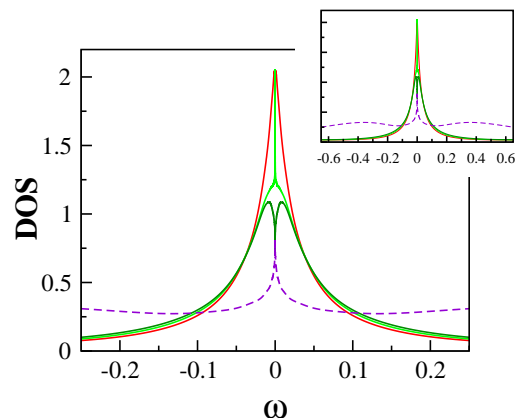


FIG. 6 Impurity spectral function with a rigid bath characterized by a flat density of states (no DMFT self-consistency) across the critical point: the curves from top to bottom correspond to the evolution from the Kondo screened regime towards the pseudogap regime. The dotted line is the spectral function deep inside the non-Fermi-liquid phase  $J \gg T_K$ . The top inset shows the same curves plotted on a larger energy range, where the pseudogap of the dotted line is visible. The Fermi liquid behavior corresponds to the normal state of the SCS superconducting phase for  $J < J_{cp}$  (analogous to the overdoped regime of cuprates) whereas the pseudogap behavior corresponds to the SCS normal state for  $J > J_{cp}$  (analogous to the underdoped cuprates). Figure from De Leo and Fabrizio (2005).

spin  $S = 1/2$  also carries orbital momentum  $L = 1$ , which corresponds to an overscreened non-Fermi liquid situation (De Leo and Fabrizio, 2005). In this regime, it was predicted that the impurity contributions to the specific-heat coefficient and to the pair susceptibility in the  $s$ -wave channel (14) diverge as  $T^{-1/5}$  at low temperature  $T$ . In addition, the conduction electron scattering rate has a non-analytic temperature-behavior  $T^{2/5}$ . The local response functions to either a quadrupolar field, which splits the orbital degeneracy, or to a magnetic field which polarizes both spins and orbitals also diverge as  $T^{-1/5}$ . The two phases, the Kondo screened phase and the pseudogap phase, are separated by a critical point at  $J = J_{cp} \simeq T_K$ . It is endowed with a finite entropy  $1/2 \ln 3$ , and with a divergent superconducting susceptibility with an exponent  $1/3$ . As shown in Fig. 6, the single-particle spectral function displays strong deviations from a normal metal in the pseudogap phase and at the critical point.

Near this critical point it has been found that the low-energy dynamics around the impurity is controlled by two separate energy scales (De Leo and Fabrizio, 2005),  $T_+$  and  $T_-$ , whose behavior is very different as a function of increasing  $U/W$ . A higher energy scale  $T_+$  is set by the critical  $J_{cp} \sim T_K$  and represents the width of a broad incoherent resonance; it evolves smoothly and uneventfully as the critical point is crossed (See Fig. 6). A lower energy scale  $T_- \propto |J - T_K|^3$  measures instead the distance from the critical point, and leads simultaneously to

<sup>3</sup> Note that the high-energy Hubbard bands are unaffected by the small attraction  $J$ ; superconductivity is just a matter of quasiparticles (Capone *et al.*, 2002). Therefore, a quasiparticle attraction exceeding their bandwidth cannot correspond to an instability towards a Mott insulator, which must involve also the Hubbard bands, but at most towards a breakdown of a quasiparticle-based Fermi liquid.

a narrow resonance in the Fermi-liquid region, and to an equally narrow spectral density dip (the “pseudogap”) in the pseudogap phase (De Leo and Fabrizio, 2005). Since in this phase the impurity still carries a residual spin-1/2, there remains a finite value of the spectral function at the chemical potential, and the gap is not complete. The pseudogap widens if  $J$  is increased, and the cusp-like dip in the impurity spectral function smoothly turns into a cusp-like peak, the value at the chemical potential staying fixed and constant. This behavior is shown by the dotted curve in Fig. 6 corresponding to a very large pseudogap (see top inset), possessing a very tiny peak at the chemical potential. This indicates the existence of yet another energy scale besides  $T_+$  and  $T_-$  that sets the width of the cusp peak.

### B. Anderson Impurity with a Self-Consistent Bath in DMFT

The rigid bath AIM behavior and its critical point briefly reviewed above provide a guide to the DMFT results once the impurity-bath coupling is self-consistently determined. First of all, since  $T_K$  coincides within DMFT with the renormalized  $ZW$  which in turn vanishes when the continuous Mott transition is approached, the impurity critical point is inevitably met before the metal insulator transition as  $U/W$  is increased, at some  $U_{cp} \lesssim U_c$ . This entails several important consequences:

- The normal state may be a Fermi liquid only far below the continuous metal insulator transition, such as perhaps may be the case in the non-expanded fullerenes. Expanded compounds on the other hand are expected to have a non-Fermi-liquid normal state, and eventually a pseudogap, possibly developing before the first order transition to the anti-ferromagnetic insulator.
- The SCS superconducting pocket near the Mott transition reflects the leading instability of the impurity critical point. In other words SCS superconductivity is the way in which the lattice model responds to impurity criticality and avoids it.
- The lower energy scale vanishes right at the critical point,  $T_- = 0$ . Here  $T_+ \simeq J$  thus remains as the only energy scale controlling the magnitude of the superconducting energy gap. Away from  $U = U_{cp}$ ,  $T_- \neq 0$ , and the amplitude of the superconducting gap should decrease monotonically with  $(T_+ - T_-)/T_+$  (Capone *et al.*, 2004), since  $T_-$  cut-offs the local pairing instability. Therefore the gap should be maximum right at the impurity critical point (the top of the dome).
- Even though the normal phase is non-Fermi liquid, well defined Bogoliubov quasiparticles should exist inside the SCS superconducting pocket.

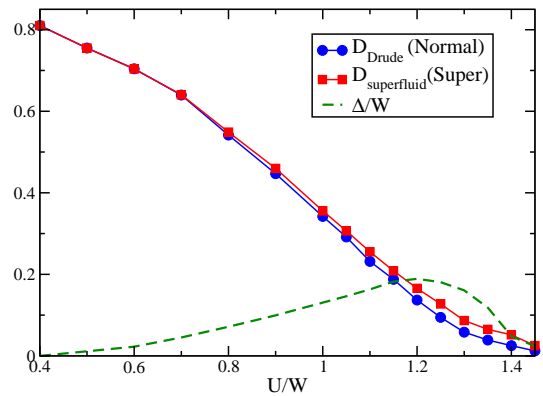


FIG. 7 Calculated weights of the zero-frequency delta-function contribution to the optical conductivity for the superconducting phase (superfluid stiffness, squares) and the normal phase (Drude weight, circles). The zero-frequency anomalous self-energy is also plotted. Note the higher values in the SCS superconductor, relative to the nonsuperconducting metal phase.

The last statement comes from the fact that, at the impurity critical point, superconductivity provides a new screening channel which helps the system get rid of the finite residual entropy at the critical point, thus eliminating non-Fermi liquid singularities (De Leo and Fabrizio, 2005; Schirò *et al.*, 2008).

The role of superconductivity as a novel screening channel close to the impurity model critical point should reflect, in the lattice model, into a gain of band energy (the tight binding “kinetic energy”) at the onset of superconductivity. Owing to a sum rule connecting kinetic energy and zero-frequency optical conductivity (sometimes referred to as “Drude weight”) (Scalapino *et al.*, 1993) the onset of SCS superconductivity close to the Mott transition should lead to a Drude weight increase. This prediction is well borne out by the full DMFT solution of our Hamiltonian. In Fig. 7 we plot the  $\omega = 0$  (d.c.) optical conductivity of our model superconductor (where it coincides with the superfluid stiffness), defined by (Toschi *et al.*, 2005)

$$D_s = -E_{kin} + \chi_{jj}(\mathbf{q} \rightarrow 0, \Omega = 0), \quad (16)$$

where  $E_{kin}$  is the kinetic energy and  $\chi_{jj}$  the static limit of the paramagnetic part of the electromagnetic kernel

$$\chi_{jj} = \frac{2}{\beta} \sum_n \int d\epsilon N(\epsilon) V(\epsilon) \times [G(\epsilon, \omega_n) G^*(\epsilon, \omega_n) + F(\epsilon, \omega_n) F(\epsilon, \omega_n)], \quad (17)$$

where  $V(\epsilon) = (4t^2 - \epsilon^2)/3$  is the current vertex in the Bethe lattice, while  $G(\epsilon, \omega_n)$  and  $F(\epsilon, \omega_n)$  are the normal and anomalous lattice Green functions, respectively. In the same figure we also plot the zero-frequency d.c. conductivity (the Drude weight) of the underlying metastable solution where superconductivity is inhibited,

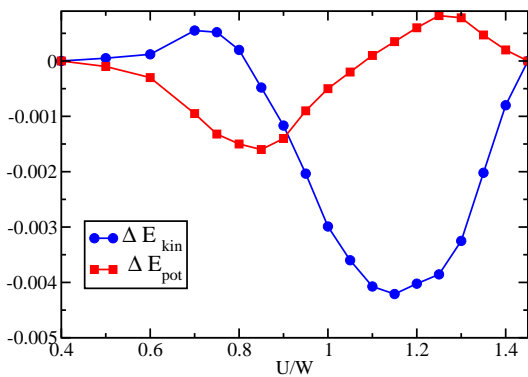


FIG. 8 Energetic balance underlying superconductivity.  $\Delta E_{pot} = E_{pot}^S - E_{pot}^N$  is the difference between the potential energies of the superconducting and the normal solution, while  $\Delta E_{kin} = E_{kin}^S - E_{kin}^N$  is the same difference between the kinetic energies of the two solutions.

this state meant to provide a cartoon of the real normal phase above  $T_c$ . The Drude weight is given by Eq. (16) and (17) with  $F(\epsilon, \omega_n) \equiv 0$ . Upon entering the SCS dome from the low  $U/W$  side, the superconducting phase initially loses kinetic energy over the normal state as in ordinary BCS theory. However, upon increasing  $U/W$  at and beyond the dome maximum, the loss reverts over to a gain, and indeed most of the SCS superconducting pocket is predicted to have a larger weight of the zero-frequency optical absorption than the non superconducting state. The same behavior is displayed (Fig. 8) by the energy balance between the two solutions. Only far below the Mott transition the superconductor is stabilized by a potential energy gain, as is the case in BCS theory. In the pseudogap regime, corresponding to the expanded fullerenes near the Mott transition, the stabilization is associated with a kinetic energy gain.

A similar phenomenon is well known in the optical conductivity of high- $T_c$  copper oxides (Carbone *et al.*, 2006). Our calculations show that an increase in the zero-frequency optical conductivity or a kinetic energy gain do not actually exclude an electron-phonon pairing mechanism, but rather demonstrates the key importance of strong electronic correlations. Thanks to pairing, the motion of carriers in the superconducting phase is facilitated with respect to the pseudogap nonsuperconducting metal. In that anomalous metal – a non Fermi liquid – the interaction constraints jam the free propagation of quasiparticles, causing a kinetic energy cost, partly released with the onset of superconductivity. It would be of extreme interest if the optical conductivity increase demonstrated in cuprates could be investigated in fullerenes, both regular and expanded, since that would help discriminate between conventional BCS and SCS.

## V. DISCUSSION OF EXPERIMENTAL PROBES

In the following we discuss whether and how the dominance of strong correlation we propose for the superconducting fullerenes can be reconciled with the list of experimental facts given earlier, apparently supporting a conventional BCS behavior. The first quantity we discuss is the specific heat jump at  $T_c$ . Within BCS theory, the specific heat jump  $\Delta C_V$  at  $T_c$  is approximately

$$\frac{\Delta C_V}{T_c} \simeq 1.52 \gamma_*, \quad (18)$$

where  $\gamma_*$  is the specific heat coefficient of the metallic phase ( $C_V = \gamma_* T$ ), proportional to the mass enhancement  $m^*/m$ , in our case  $1/Z$ . The measured specific heat jump leads, through (18), to an estimate of  $\gamma_* \simeq 3\gamma_0$ . This is indeed a rather low and regular value which has been commonly advocated as evidence of weak correlations in fullerenes. However, the standard argument only holds provided the normal phase is Fermi-liquid, which is not applicable close to a Mott transition, independently of any models.

In Fig. 9 we plot the jump in  $C_V$  at  $T_c$  for increasing  $U/W$ , compared with the Fermi-liquid estimate  $1/Z$ .<sup>4</sup> After a region where the calculated quantity closely follows  $1/Z$ ,  $\Delta C_V/T_c$  flattens out and stays roughly con-

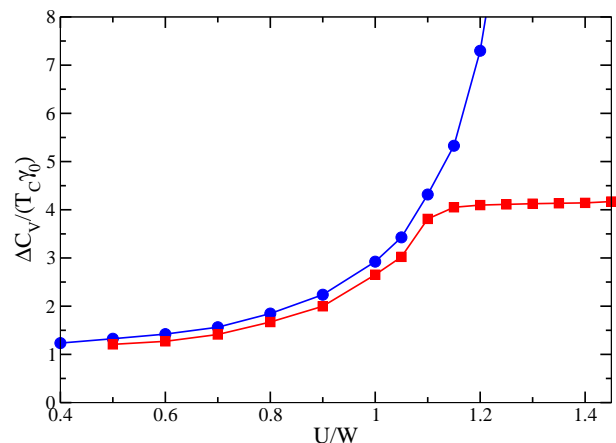


FIG. 9 Specific heat jump, in units of  $T_c$ ,  $\gamma_0$ , as function of  $U/W$ . For comparison we also show the behavior of  $1/Z(U)$ , which should correspond to the same quantity if Fermi liquid theory were valid.

<sup>4</sup> As mentioned in Sec. III.A, for the present three-orbital model it has not been practical to include in Eq. (6) a number of excited states sufficient to make the truncation error in the Green's function negligible. For the data reported in Fig. 9 we have an average error of 3-4% which does not allow us to determine  $T_c$  with sufficient accuracy. Yet, the jump of the specific heat relative to  $T_c$  turns out to be almost independent on the truncation error and on the details of the calculations.

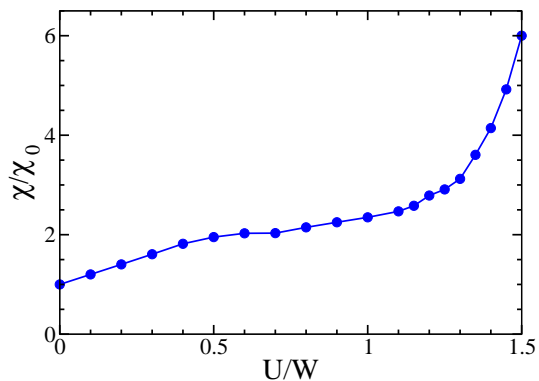


FIG. 10 Normal-phase uniform magnetic susceptibility  $\chi$  normalized to the non-interacting value  $\chi_0$ . For  $U = 0$ ,  $\chi \simeq \chi_0$ , the difference being extremely small since  $J \ll W$ . The plateau between  $U/W = 0.5$  and  $1$  signals the effective crossover from a Fermi liquid with  $S = 3/2$  per site, to a non Fermi liquid with  $S = 1/2$  per site.

stant around  $4\gamma_0$  up to the Mott transition, despite a diverging  $1/Z$  (See Fig. 9). This shows that the energy scale that controls the superconducting instability is constant near the Mott transition, consistent with the single-impurity prediction that this scale should be identified by  $T_+$ , a quantity of order  $J$ . The bottom line conclusion here is that a normally sized specific-heat jump does not imply BCS superconductivity in fullerenes.

Another physical quantity which seemingly pointed towards weak correlations in fullerenes is the magnetic susceptibility measured in the normal phase, apparently consistent with a weakly correlated Fermi liquid and a Stoner enhancement of about a factor 2 to 3. This argument again becomes inconclusive once the Fermi-liquid scenario is abandoned. In Fig. 10 we plot as function of  $U/W$  the uniform magnetic susceptibility in the normal phase calculated by DMFT. After an initial Stoner enhancement at small  $U/W$ , the susceptibility flattens out and remains almost constant before a rapid growth which takes place extremely close to the Mott transition. In the plateau region the susceptibility enhancement of a factor between 2 and 3 with respect to  $U = 0$ , surprisingly close to the experimental enhancement, covering the whole superconducting domain. Physically, the origin of this susceptibility plateau for increasing  $U$  is quite instructive. It corresponds to the gradual crossover of the maximum spin available at each site from  $S = 3/2$  in the Fermi liquid at small  $U < U_{cp}$  (Kondo screened AIM) to  $S = 1/2$  near Mott and large  $U > U_{cp}$ , where Fermi liquid behavior is lost. In essence, at large  $U$  each molecule is effectively in a (dynamically) JT distorted state, where two out of three electrons are spin paired (Auerbach *et al.*, 1994). We are thus led to conclude that the relatively weak observed enhancement of susceptibility does not correspond at all to a Stoner enhanced, weakly correlated Fermi liquid – in fact quasiparticles do not even exist in most of the plateau region.

Finally, we wish to address signatures of the strongly

correlated scenario which we expect should show up in important spectroscopies including the tunneling I-V characteristics and angle resolved photoemission spectroscopy (ARPES). This is initially embarrassing on two accounts. First, ARPES spectroscopies are  $\mathbf{k}$ -vector resolved, whereas in DMFT we do not have access to any spatial structure. Second, tunneling spectroscopies are extremely well resolved near zero voltage, whereas our Lanczos method yields a much poorer spectral function resolution in this region.

Let us address tunneling first. Although Fig. 6 refers to the impurity  $C_{60}^{3-}$  molecule, we believe that similar features would remain after full DMFT self-consistency in the normal phase – if we only had a better low-frequency numerical resolution than we presently have. Hence, we suggest that tunneling I-V spectra of expanded fullerenes be measured and examined, in order to bring out the expected rich structure of the kind sketched in Fig. 6.

Next, let us consider photoelectron spectroscopy. Again according to the single-impurity analysis (De Leo and Fabrizio, 2005), the imaginary part of the single-particle self-energy should be finite and of order  $T_+$  almost everywhere in the non-Fermi liquid normal phase above  $T_c$ . This has the following implications for ARPES:

- the fullerene photoemission spectrum should show  $t_{1u}$  bands dispersing in the Brillouin zone with nonzero bandwidth, governed by the energy scale  $T_+$ . The value of  $T_+$  decreases with increasing  $U/W$  (increasing expansion), from  $W$  at  $U = 0$  to (larger than)  $J$  at the Mott transition;
- there should be a spectral peak broadening of the same order of magnitude  $T_+$  as the apparent  $\mathbf{k}$ -resolved band dispersion. In particular the broadening should remain constant approaching the Fermi surface – unlike a Fermi liquid phase where quasi-particle peaks become narrower and narrower.

The momentum-independence of the DMFT self-energy implies that, in this approximation, the  $\mathbf{k}$ -modulation of the electronic dispersion is assumed to remain unaffected by interactions. Within this assumption and without requiring too high frequency-accuracy, we can compute a toy  $\mathbf{k}$ -resolved spectral function according to

$$A(k, \omega) = -\frac{1}{\pi} \text{Im} \frac{1}{\omega - \varepsilon_{\mathbf{k}} - \Sigma_{DMFT}(\omega)}, \quad (19)$$

where  $\varepsilon_{\mathbf{k}}$  is the non interacting dispersion and  $\Sigma_{DMFT}(\omega)$  is the DMFT self-energy calculated with a finite number of baths. The effect of the local self-energy will be to change the effective bandwidth and to give rise to finite lifetime effects, even if the  $\mathbf{k}$ -modulation of the dispersion is unrenormalized. For our Bethe lattice,

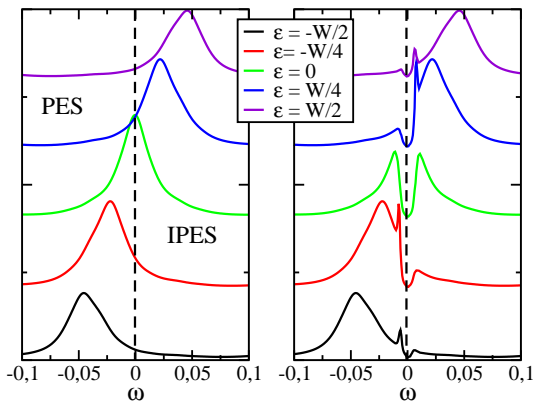


FIG. 11 Simulated photoemission spectra elaborated from the DMFT result in the normal phase. The left panel refers to  $U/W = 1.1$  (corresponding to unexpanded fullerides), while the right panel is for  $U/W = 1.3$  (corresponding to expanded fullerides).

there is no straightforward definition of momentum, and we remedy that by computing  $A(\varepsilon, \omega)$ , which corresponds to Eq. (19) with  $\varepsilon_{\mathbf{k}} \rightarrow \varepsilon$ .

In Fig. 11 we show theoretical ARPES results for some choices of  $\varepsilon$  obtained by using the DMFT self-energy for temperatures above  $T_c$ , both for a value of  $U/W = 1.1$  which lies close to the maximum of the superconducting dome, but still on the less correlated side, corresponding to unexpanded (or moderately expanded) fullerides, and for a value which lies in the downward branch of the dome ( $U/W = 1.3$ ), corresponding to a very expanded fulleride. We note in both cases the existence of an incoherent low-energy feature dispersing with a reduced but nonzero electron bandwidth of  $0.1 W$ . In the expanded case the pseudogap feature is clearly present.

Recent photoemission spectra of  $K_3C_{60}$  (Goldoni, 2007) indicate an overall dispersion bandwidth of about 160 meV, about a quarter of the bare calculated bandwidth in the local-density approximation. The experimental spectral peak does not show the usual Fermi-liquid-like narrowing on approaching the Fermi level, a fact which is in agreement with our expectation for a non Fermi liquid (although a non expanded fulleride like  $K_3C_{60}$  probably lies at the beginning of the SCS dome, where deviations from Fermi liquid are not massive). Experimentally the peak does not appear to cross the Fermi level, and the intensity instead drops, suggestive of a pseudogap. Unfortunately the spectrum shows very strong vibronic effects, reflecting the retarded strong electron Jahn Teller coupling. This aspect is not covered by our unretarded approximation, but it heavily affects the line shape and hampers the extraction of purely electronic features. Treatment of the vibronic effects, and a quantitative description of dispersion, will require abandoning in the future our approximation of infinitely fast phonon dynamics, as well as a possible extension to cluster extensions of DMFT which allow for different renormalizations of different momenta (Hettler *et al.*, 2000).

## VI. CONCLUSIONS

Summarizing, we addressed the apparently contradictory properties of expanded trivalent fullerides superconductors and insulators – and to some extent of the whole family of fullerides – and presented a theoretical scenario emphasizing the role of strong electron correlations. That is especially designed and appropriate for the more expanded members of the family, such as  $(NH_3)_xNaK_2C_{60}$ ,  $Li_3C_{60}$ ,  $Cs_{3-x}K_xC_{60}$  and  $Cs_{3-x}Rb_xC_{60}$ , and the recently discovered A15  $Cs_3C_{60}$  that are near or past the Mott transition.

Our model explains the dome-shaped increase and subsequent decrease of  $T_c$  upon expansion of the lattice spacing in fullerides; the coexistence of metallic behavior and of Mott insulator features such as the large NMR spin gap in all fullerides, and the  $S = 1/2$  spin in the insulating state (identified as a Mott-Jahn-Teller insulator). It explains why the  $s$ -wave  $T_c$  can be as high as 40 K even though the Coulomb interaction strength is prohibitive, and why  $T_c$  does not automatically decrease upon increase of  $U/W$ . It also accounts for more standard observations, such as regular specific heat jumps and moderately high spin susceptibilities, facts that were so far construed as evidence for conventional BCS superconductivity.

Besides those listed in the previous Section, one can anticipate a number of additional experiments that could provide “smoking gun” evidence for strongly correlated superconductivity in fullerides. The tunneling  $I$ - $V$  characteristics observable, e.g., by a scanning tunneling spectroscopy tip should, in an expanded fulleride, develop the low energy features typical of the Kondo impurity spectral function. The isotope effect upon carbon substitution should also behave very unconventionally, and eventually get smaller as the superconducting dome is passed and the Mott transition is approached upon expansion. In this regime, as the quasiparticle bandwidth  $ZW$  gradually falls below the typical energy  $\hbar\omega$  of an increasing fraction of the eight  $H_g$  Jahn Teller modes, the associated retardation effect should in fact disappear. The expanded fullerides and related materials, clearly not enough investigated so far, deserve in our view the strongest experimental attention. They combine elements that make them members at large of the high temperature superconductor family. They combine neighborhood of the Mott transition and predominance of strong electron correlations, with conventional elements such as electron-phonon  $s$ -wave pairing, that are typical of BCS systems. Our study identifies a pseudogap and other features in the  $IV$  tunneling spectrum, an increase of zero-frequency optical weight in the optical response of the superconducting phase, and the emergence of two separate energy scales in ARPES as the most urgent experimental undertakings that could confirm or falsify our claims.

## Acknowledgments

E.T. thanks Kosmas Prassides, Andrea Goldoni, and Mauro Ricco' for information and discussion about fullerenes and again K.P. for providing us with Fig. 1. M.C. acknowledges discussions with A. Toschi. Work in SISSA was sponsored by PRIN Cofin 2006022847, as well as by INFN/CNR "Iniziativa trasversale calcolo parallelo". Work in Rome was sponsored by PRIN Cofin 200522492.

## References

- Abrikosov, A. A., L. P. Gor'kov, , and I. E. Dzyaloshinskii, 1965, *Quantum field theoretical methods in statistical physics* (Pergamon).
- Anderson, P. W., 1987, *Science* **235**, 1196.
- Auerbach, A., N. Manini, and E. Tosatti, 1994, *Phys. Rev. B* **49**, 12998.
- Bardeen, J., L. N. Cooper, and J. R. Schrieffer, 1957a, *Phys. Rev.* **106**, 162.
- Bardeen, J., L. N. Cooper, and J. R. Schrieffer, 1957b, *Phys. Rev.* **108**, 1175.
- Baskaran, G., and E. Tosatti, 1991, *Curr. Sci.* **61**, 33.
- Bennemann, K. H., and J. B. Ketterson (eds.), 2008, *Superconductivity* (Springer).
- Brouet, V., H. Alloul, S. Garaj, and L. Forró, 2002a, *Phys. Rev. B* **66**, 155122.
- Brouet, V., H. Alloul, S. Garaj, and L. Forró, 2002b, *Phys. Rev. B* **66**, 155124.
- Burkhardt, G. J., and C. Meingast, 1996, *Phys. Rev. B* **54**, R6865.
- Capone, M., M. Fabrizio, C. Castellani, and E. Tosatti, 2002, *Science* **296**, 2364.
- Capone, M., M. Fabrizio, C. Castellani, and E. Tosatti, 2004, *Phys. Rev. Lett.* **93**, 047001.
- Capone, M., M. Fabrizio, P. Giannozzi, and E. Tosatti, 2000, *Phys. Rev. B* **62**, 7619.
- Capone, M., M. Fabrizio, and E. Tosatti, 2001, *Phys. Rev. Lett.* **86**, 5361.
- Capone, M., L. de' Medici, and A. Georges, 2007, *Phys. Rev. B* **76**, 245116.
- Cappelluti, E., C. Grimaldi, L. Pietronero, and S. Strässler, 2000, *Phys. Rev. Lett.* **85**, 4771.
- Carbone, F., A. B. Kuzmenko, H. J. A. Molegraaf, E. van Heumen, E. Giannini, and D. van der Marel, 2006, *Phys. Rev. B* **74**, 024502, and references therein.
- Chakravarty, S., M. Gelfand, , and S. Kivelson, 1991, *Science* **254**, 970.
- Chakravarty, S., and S. Kivelson, 1991, *Phys. Rev. B* **64**, 064511.
- Dahlke, P., M. S. Denning, P. F. Henry, and M. J. Rosseinsky, 2000, *J. Am. Chem. Soc.* **122**, 12352.
- Dahlke, P., and M. J. Rosseinsky, 2002, *Chem. Mater.* **14**, 1285.
- De Leo, L., and M. Fabrizio, 2005, *Phys. Rev. Lett.* **94**, 236401.
- Durand, P., G. R. Darling, Y. Dubitsky, A. Zaopo, and M. J. Rosseinsky, 2003, *Nature Materials* **2**, 605.
- Eliashberg, G. M., 1960, *Zh. Eksp. Teor. Fiz.* **38**, 966, ; *ibid.* **39**, 1437 (1960) [*Sov. Phys. JETP* **11**, 696 (1960); **12**, 1000 (1960)].
- Erwin, S. C., 1993, in *Buckminsterfullerenes*, edited by W. Billups and M. Ciufolini (VHC, New York), p. 217.
- Fabrizio, M., A. F. Ho, L. De Leo, and G. E. Santoro, 2003, *Phys. Rev. Lett.* **91**(24), 246402.
- Fabrizio, M., and E. Tosatti, 1997, *Phys. Rev. B* **55**, 13465.
- Ganin, A. Y., Y. Takahashi, Y. Z. Khimyak, S. Margadonna, A. Tamai, M. J. Rosseinsky, and K. Prassides, 2008, *Nature Materials* **7**, 367.
- Georges, A., G. Kotliar, W. Krauth, and M. J. Rozenberg, 1996, *Rev. Mod. Phys.* **68**, 13.
- Goldoni, A., 2007, unpublished.
- Granath, M., and S. Östlund, 2003, *Phys. Rev. B* **68**, 205107.
- Gunnarsson, O., 1997, *Rev. Mod. Phys.* **69**, 575.
- Gunnarsson, O., 2004, *Alkali-doped Fullerenes. Narrow-band solids with unusual properties* (World Scientific, Singapore).
- Gunnarsson, O., H. Handschuh, P. S. Bechthold, B. Kessler, G. Ganterör, and W. Eberhardt, 1995, *Phys. Rev. Lett.* **74**, 1875.
- Gutzwiller, M. C., 1963, *Phys. Rev. Lett.* **10**, 159.
- Han, J. E., O. Gunnarsson, and V. H. Crespi, 2003, *Phys. Rev. Lett.* **90**, 167006.
- Hettler, M. H., M. Mukherjee, M. Jarrell, and H. R. Krishnamurthy, 2000, *Phys. Rev. B* **61**, 12739.
- Hewson, A., 1997, *The Kondo Problem to Heavy Fermions* (Cambridge University Press).
- Huq, A., and P. W. Stephens, 2006, *Phys. Rev. B* **74**, 075424.
- Iwasa, Y., and T. Takenobu, 2003, *J. Phys.: Condens. Matter* **15**, R495, and references therein.
- Kitano, H., R. Matsuo, K. Miwa, A. Maeda, T. Takenobu, Y. Iwasa, and T. Mitani, 2002, *Phys. Rev. Lett.* **88**, 096401.
- Klupp, G., K. Kamarás, N. M. Nemes, C. M. Brown, and J. Leão, 2006, *Phys. Rev. B* **73**, 085415.
- Knupfer, M., and J. Fink, 1997, *Phys. Rev. Lett.* **79**, 2714.
- Kortan, A. R., M. J. Rosseinsky, S. J. Duclos, A. M. Mujica, R. C. Haddon, D. W. Murphy, A. V. Makhija, S. M. Zahurak, and K. B. Lyons, 1992, *Phys. Rev. Lett.* **68**, 1058.
- Landau, L. D., and E. M. Lifshitz, 1958, *Quantum Mechanics: non-relativistic theory* (Pergamon Press, Inc., New York).
- Lannoo, M., G. Baraff, M. Schluter, and D. Tomanek, 1991, *Phys. Rev. B* **44**, 12106.
- Lof, R., M. van Veenendaal, B. Koopmans, H. Jonkman, and G. Sawatzky, 1992, *Phys. Rev. Lett.* **68**, 3924.
- Lüders, M., A. Bordon, N. Manini, A. D. Corso, M. Fabrizio, and E. Tosatti, 2002, *Phil. Mag. B* **82**, 1611.
- Martin, R. L., and J. P. Ritchie, 1993, *Phys. Rev. B* **48**, 4845.
- Micnas, R., J. Ranninger, and S. Robaszkiewicz, 1990, *Rev. Mod. Phys.* **62**, 113.
- Migdal, A. B., 1958, *Zh. Eksp. Teor. Fiz.* **34**, 1438, [*Sov. Phys. JETP* **7**, 996 (1958)].
- Mott, N. F., 1990, *Metal Insulator Transition* (Taylor and Francis, London).
- Onnes, H. K., 1911, *Leiden Comm.* **120b**, **122b**, **124c**.
- Palstra, T. T. M., O. Zhou, Y. Iwasa, P. E. Sulewski, R. M. Fleming, and B. R. Zegarski, 1995, *Sol. St. Comm.* **93**, 327.
- Parks, R. D. (ed.), 1969, *Superconductivity* (Marcel Dekker, New York).
- Prassides, K., S. Margadonna, D. Arcon, A. Lappas, H. Shimoda, and Y. Iwasa, 1999, *J. Am. Chem. Soc.* **121**, 11227.
- Ramirez, A. P., 1994, *Superconductivity Review* **1**, 1.
- Riccó, M., G. Fumera, T. Shiroka, O. Ligabue, C. Bucci, and F. Bolzoni, 2003, *Phys. Rev. B* **68**, 035102.
- Robert, J., P. Petit, T. Yildirim, and J. E. Fischer, 1998, *Phys. Rev. B* **57**, 1226.

- Satpathy, S., V. P. Antropov, O. K. Andersen, O. Jepsen, O. Gunnarsson, and A. I. Liechtenstein, 1992, *Phys. Rev. B* **46**(3), 1773.
- Scalapino, D. J., S. R. White, and S. Zhang, 1993, *Phys. Rev. B* **47**(13), 7995.
- Schirò, M., M. Capone, M. Fabrizio, and C. Castellani, 2008, *Phys. Rev. B* **77**, 104522.
- Thier, K.-F., G. Zimmer, M. Mehring, and F. Rachdi, 1995, in *Physics and Chemistry of Fullerenes and Derivatives*, edited by H. Kuzmany, O. Fink, M. Mehring, and S. Roth (World Scientific, Singapore), p. 432.
- Toschi, A., M. Capone, and C. Castellani, 2005, *Phys. Rev. B* **72**, 235118.
- Varma, C., J. Zaanen, and K. Raghavachari, 1991, *Science* **254**, 989.
- Wachowiak, A., R. Yamachika, K. H. Khoo, Y. Wang, M. Grobis, D.-H. Lee, S. G. Louie, and M. F. Crommie, 2005, *Science* **310**, 468.
- Yildirim, Y., J. E. Fisher, R. Dinnebier, P. W. Stephens, and C. L. Lin, 1995, *Sol. St. Comm.* **93**, 295.
- Zhou, O., T. T. M. Palstra, Y. Iwasa, R. M. Fleming, A. F. Hebard, and P. E. Sulewski, 1995, *Phys. Rev. B* **52**, 483.